Eur. Phys. J. C (2016) 76:657
DOI 10.1140/epjc/s10052-016-4515-9

THE EUROPEAN PHYSICAL JOURNAL C

Regular Article - Theoretical Physics

Reanalysis of $X(4140)$ as axial-vector tetraquark state with QCD sum rules

Zhi-Gang Wang[a]

Department of Physics, North China Electric Power University, Baoding 071003, People's Republic of China

Received: 9 September 2016 / Accepted: 14 November 2016 / Published online: 29 November 2016

Abstract In this article, we take $X(4140)$ as the diquark–antidiquark type $cs\bar{c}\bar{s}$ tetraquark state with $J^{PC}=1^{++}$, and we study the mass and pole residue with the QCD sum rules in detail by constructing two types of interpolating currents. The numerical results $M_{X_{L,+}}=3.95\pm0.09\,\text{GeV}$ and $M_{X_{H,+}}=5.00\pm0.10\,\text{GeV}$ disfavor assigning the $X(4140)$ to the $J^{PC}=1^{++}$ diquark–antidiquark type $cs\bar{c}\bar{s}$ tetraquark state. Moreover, we obtain the masses of the $J^{PC}=1^{+-}$ diquark–antidiquark type $cs\bar{c}\bar{s}$ tetraquark states as a byproduct. The present predictions can be confronted to the experimental data in the future.

1 Introduction

In 2009, the CDF collaboration observed $X(4140)$ for the first time in the $J/\psi\phi$ invariant mass distribution in the exclusive $B^+\to J/\psi\,\phi K^+$ decays in $p\bar{p}$ collisions at $\sqrt{s}=1.96\,\text{TeV}$ with a statistical significance of more than 3.8σ [1]. In 2011, the CDF collaboration confirmed $X(4140)$ in the $B^\pm\to J/\psi\,\phi K^\pm$ decays with a statistical significance of more than 5σ, and observed evidence for $X(4274)$ in the $J/\psi\phi$ invariant mass distribution with a statistical significance of about 3.1σ [2]. In 2013, the CMS collaboration confirmed $X(4140)$ in the $B^\pm\to J/\psi\phi K^\pm$ decays in pp collisions at $\sqrt{s}=7\,\text{TeV}$ collected with the CMS detector at the LHC with a statistical significance of more than 5σ [3], the D0 collaboration confirmed $X(4140)$ in the $B^+\to J/\psi\phi K^+$ decays with a statistical significance of 3.1σ based on the data sample corresponding to an integrated luminosity of $10.4\,\text{fb}^{-1}$ of $p\bar{p}$ collisions at $\sqrt{s}=1.96\,\text{TeV}$ [4]. There have been several possible assignments for $X(4140)$ since its first observation by the CDF collaboration [1], such as a molecular state [5–13], a tetraquark state [14–18], a hybrid state [19–21] or a rescattering effect [22,23].

Recently, the LHCb collaboration performed the first full amplitude analysis of the decays $B^+\to J/\psi\phi K^+$ with $J/\psi\to\mu^+\mu^-$, $\phi\to K^+K^-$ with a data sample corresponding to an integrated luminosity of $3\,\text{fb}^{-1}$ of pp collision data collected at $\sqrt{s}=7$ and $8\,\text{TeV}$ with the LHCb detector, and observed that the data cannot be described by a model that contains only excited kaon states decaying into ϕK^+ [24,25]. The LHCb collaboration confirmed the two old particles $X(4140)$ and $X(4274)$ in the $J/\psi\phi$ invariant mass distributions with statistical significances 8.4σ and 6.0σ, respectively, and determined the spin-parity-change-conjugation to be $J^{PC}=1^{++}$ with statistical significances of 5.7σ and 5.8σ, respectively [24,25]. Moreover, the LHCb collaboration observed the two new particles $X(4500)$ and $X(4700)$ in the $J/\psi\phi$ invariant mass distributions with statistical significances of 6.1σ and 5.6σ, respectively, and determined the spin-parity-change-conjugation to be $J^{PC}=0^{++}$ with statistical significances 4.0σ and 4.5σ, respectively [24,25]. The measured Breit–Wigner masses and widths are

$$\begin{aligned}
X(4140):&\ M=4146.5\pm4.5^{+4.6}_{-2.8}\,\text{MeV},\\
&\ \Gamma=83\pm21^{+21}_{-14}\,\text{MeV},\\
X(4274):&\ M=4273.3\pm8.3^{+17.2}_{-3.6}\,\text{MeV},\\
&\ \Gamma=56\pm11^{+8}_{-11}\,\text{MeV},\\
X(4500):&\ M=4506\pm11^{+12}_{-15}\,\text{MeV},\\
&\ \Gamma=92\pm21^{+21}_{-20}\,\text{MeV},\\
X(4700):&\ M=4704\pm10^{+14}_{-24}\,\text{MeV},\\
&\ \Gamma=120\pm31^{+42}_{-33}\,\text{MeV}.
\end{aligned}\tag{1}$$

The LHCb collaboration determined the quantum numbers of the $X(4140)$ to be $J^{PC}=1^{++}$, which rules out the 0^{++} or 2^{++} $D_s^{*+}D_s^{*-}$ molecule assignment. In the constituent diquark model, the masses of the ground state $cs\bar{c}\bar{s}$ tetraquark states with $J^{PC}=0^{-+}$, 1^{-+} are about 4.3 GeV [15], while the masses of the ground state diquark–

[a] e-mail: zgwang@aliyun.com

antidiquark type $cs\bar{c}\bar{s}$ tetraquark states with $J^{PC}=0^{++}$ and 2^{++} from the QCD sum rules are about 3.98 ± 0.08 GeV and 4.13 ± 0.08 GeV, respectively [17]. In Ref. [18], Lebed and Polosa propose that $X(3915)$ is the ground state scalar–diquark–scalar–antidiquark type scalar $cs\bar{c}\bar{s}$ tetraquark state according to lacking of the observed decays to the final states $D\bar{D}$ and $D^*\bar{D}^*$, and they attribute the only known decay to the final state $J/\psi\omega$ to the $\omega-\phi$ mixing effect. In Ref. [26], we tentatively assign $X(3915)$ and $X(4500)$ to the ground state and the first radial excited state of the axial-vector–diquark–axial-vector–antidiquark type scalar $cs\bar{c}\bar{s}$ tetraquark states, respectively, and we study their masses and pole residues in detail with the QCD sum rules, and obtain the values

$$\begin{aligned} M_{X(3915)} &= 3.92^{+0.19}_{-0.18}\,\text{GeV}, \quad \text{Experimental value,} \\ &\quad 3918.4\pm1.9\,\text{MeV}\,[27], \\ M_{X(4500)} &= 4.50^{+0.08}_{-0.09}\,\text{GeV}, \quad \text{Experimental value,} \\ &\quad 4506\pm11^{+12}_{-15}\,\text{MeV}\,[14,15], \end{aligned} \tag{2}$$

which are consistent with the experimental data. The inclusion of the first radial excited state beyond the ground state in the QCD sum rules leads to smaller ground state mass [27], which happens to lie in the same energy region as $X(3915)$. If the masses of the ground state diquark–antidiquark type 0^{++} and 2^{++} $cs\bar{c}\bar{s}$ tetraquark states are about 3.9 and 4.1 GeV, respectively, we would expect that the ground state diquark–antidiquark type 1^{++} $cs\bar{c}\bar{s}$ tetraquark state has a mass of about 3.9–4.1 GeV.

In Ref. [14], Stancu calculates the mass spectrum of the $c\bar{c}s\bar{s}$ tetraquark states within a simple quark model with chromomagnetic interaction and effective quark masses extracted from meson and baryon spectra and obtains the two lowest masses 4195 and 4356 MeV of the tetraquark states with $J^{PC}=1^{++}$. The value 4195 MeV is consistent with the experimental data $4146.5\pm4.5^{+4.6}_{-2.8}$ MeV. In the simple chromomagnetic interaction model, there are no correlated quarks or diquarks [14].

The scattering amplitude for one-gluon exchange is proportional to

$$T^a_{ki}T^a_{lj}=-\frac{1}{3}(\delta_{jk}\delta_{il}-\delta_{ik}\delta_{jl})+\frac{1}{6}(\delta_{jk}\delta_{il}+\delta_{ik}\delta_{jl}), \tag{3}$$

where the T^a is the generator of the $SU_c(3)$ gauge group, and the i, j and k, l are the color indices of the two quarks in the incoming and outgoing channels, respectively. The negative sign in front of the antisymmetric antitriplet indicates the interaction is attractive, which favors the formation of diquark states in the color antitriplet [28,29], so we usually take the diquarks in color antitriplet as the basic constituents in studying the baryon states, tetraquark states, and pentaquark states. The diquarks $\varepsilon^{ijk}q_j^TC\Gamma q_k'$ in the color antitriplet have five structures in Dirac spinor space, where the i, j, and k are color indices, $C\Gamma=C\gamma_5$, C, $C\gamma_\mu\gamma_5$, $C\gamma_\mu$ and $C\sigma_{\mu\nu}$ for the scalar, pseudoscalar, vector, axial-vector, and tensor diquarks, respectively. The stable diquark configurations are the scalar ($C\gamma_5$) and axial-vector ($C\gamma_\mu$) diquark states from the QCD sum rules [30–32], we can construct the tetraquark states using the scalar or axial-vector diquarks rather than the uncorrelated quarks to obtain the lowest masses.

In Ref. [33], we study the masses and pole residues of the axial-vector hidden-charm tetraquark states in details with the QCD sum rules, and observe that the predictions $M_{X(3872)}=3.87^{+0.09}_{-0.09}\,\text{GeV}$ and $M_{Z_c(3900)}=3.91^{+0.11}_{-0.09}\,\text{GeV}$ support assigning $X(3872)$ and $Z_c(3900)$ to the 1^{++} and 1^{+-} diquark–antidiquark type tetraquark states, respectively. If we take $X(4140)$ as the hidden-strange cousin of $X(3872)$, then the mass difference $M_{X(4140)}-M_{X(3872)}=275\,\text{MeV}$, the $SU(3)$ breaking effect is about $m_s-m_q=135\,\text{MeV}$, which is consistent with our naive expectation. In Ref. [34], Chen and Zhu obtain the value 4.07 ± 0.10 GeV for the mass of the $C\gamma_5\otimes\gamma_\mu C+C\gamma_\mu\otimes\gamma_5C$ type $cs\bar{c}\bar{s}$ tetraquark states based on the QCD sum rules, the theoretical value 4.07 ± 0.10 GeV overlaps with the experimental value $4146.5\pm4.5^{+4.6}_{-2.8}$ MeV, which supports assigning the $X(4140)$ to the axial-vector tetraquark state [35]. Although the masses of the axial-vector tetraquark states are calculated with the QCD sum rules, the routines are different [33,34]. In Ref. [33], we study the energy-scale dependence of the QCD spectral densities for the first time, and in subsequent work [36–38], we suggest an empirical energy-scale formula,

$$\mu=\sqrt{M^2_{X/Y/Z}-(2\mathbb{M}_Q)^2}, \tag{4}$$

with the effective heavy quark masses $\mathbb{M}_Q$ to determine the ideal energy scales of the QCD spectral densities of the hidden-charm and the hidden-bottom tetraquark states in the QCD sum rules.

Before the work [34], we performed a systematic study of the mass spectrum of the axial-vector hidden-charm and hidden-bottom tetraquark states using the QCD sum rules, and obtained the ground state masses $M_{cq\bar{c}\bar{q}}=4.32\pm0.18$ GeV and $M_{cs\bar{c}\bar{s}}=4.40\pm0.16$ GeV [39], and the mass breaking effect $M_{cs\bar{c}\bar{s}}-M_{cq\bar{c}\bar{q}}=80\,\text{MeV}$, which is much smaller than the experimental value $M_{X(4140)}-M_{X(3872)}=275\,\text{MeV}$. In Ref. [39], we extract the masses from the QCD spectral densities at the energy scale $\mu=1\,\text{GeV}$, which is much smaller than the optimal energy scales determined by the empirical energy-scale formula, and results in a much larger mass $M_{cq\bar{c}\bar{q}}=4.32\pm0.18$ GeV compared to the mass $M_{X(3872)/Z_c(3900)}\approx3.9$ GeV extracted at the optimal energy scales [33].

In Ref. [37], we study the masses and pole residues of the $J^{PC}=1^{-\pm}$ hidden-charm tetraquark states at the optimal energy scales with the QCD sum rules. The predicted masses

of the tetraquark states with symbolic quark structures $c\bar{c}s\bar{s}$ and $c\bar{c}(u\bar{u}+d\bar{d})/\sqrt{2}$ support assigning $Y(4660)$ to the 1^{--} diquark–antidiquark type tetraquark state, the mass difference $M_{c\bar{c}s\bar{s}}-M_{c\bar{c}(u\bar{u}+d\bar{d})/\sqrt{2}}=40\,\text{MeV}$ is even smaller compared to the value 80 MeV obtained in Ref. [39].

Now we can draw the conclusion tentatively that the QCD sum rules support smaller $SU(3)$ breaking effect than our naive expectation. It is interesting to perform detailed studies of the $X(4140)$ as the axial-vector $cs\bar{c}\bar{s}$ tetraquark state based on the QCD sum rules.

In this article, we take $X(4140)$ as the axial-vector $cs\bar{c}\bar{s}$ tetraquark state, construct the diquark–antidiquark type axial-vector currents, calculate the contributions of the vacuum condensates up to dimension 10 in the operator product expansion in a consistent way, use the empirical energy-scale formula to determine the ideal energy scales of the QCD spectral densities, and study the ground state masses and pole residues in detail with the QCD sum rules. We want to obtain additional support in assigning $X(4140)$ to the 1^{++} $cs\bar{c}\bar{s}$ tetraquark state from the QCD sum rules.

The article is arranged as follows: we derive the QCD sum rules for the masses and pole residues of the axial-vector $cs\bar{c}\bar{s}$ tetraquark states in Sect. 2; in Sect. 3, we present the numerical results and discussions; Sect. 4 is reserved for our conclusion.

2 QCD sum rules for the axial-vector $cs\bar{c}\bar{s}$ tetraquark states

In the following, we write down the two-point correlation functions $\Pi^{\pm}_{\mu\nu}(p)$ in the QCD sum rules,

$$\Pi^{\pm}_{\mu\nu}(p)=i\int \mathrm{d}^4x \mathrm{e}^{ip\cdot x}\left\langle 0|T\left\{J^{\pm}_{\mu}(x)J^{\pm\dagger}_{\nu}(0)\right\}|0\right\rangle, \tag{5}$$

where $J^{\pm}_{\mu}(x)=J^{L,\pm}_{\mu}(x)$, $J^{H,\pm}_{\mu}(x)$,

$$\begin{aligned}J^{L,\pm}_{\mu}(x)=&\frac{\epsilon^{ijk}\epsilon^{imn}}{\sqrt{2}}\left\{s^j(x)C\gamma_5c^k(x)\bar{s}^m(x)\gamma_\mu C\bar{c}^n(x)\right.\\&\left.\pm s^j(x)C\gamma_\mu c^k(x)\bar{s}^m(x)\gamma_5C\bar{c}^n(x)\right\},\end{aligned} \tag{6}$$

$$\begin{aligned}J^{H,\mp}_{\mu}(x)=&\frac{\epsilon^{ijk}\epsilon^{imn}}{\sqrt{2}}\left\{s^j(x)Cc^k(x)\bar{s}^m(x)\gamma_5\gamma_\mu C\bar{c}^n(x)\right.\\&\left.\pm s^j(x)C\gamma_\mu\gamma_5c^k(x)\bar{s}^m(x)C\bar{c}^n(x)\right\},\end{aligned} \tag{7}$$

the i,j,k,m,n are color indices, the C is the charge conjunction matrix. We choose the currents $J^{L/H,+}_{\mu}(x)$ to interpolate the $J^{PC}=1^{++}$ diquark–antidiquark type hidden-charm tetraquark states. Under a charge conjunction transform $\widehat{C}$, the currents $J^{L/H,\pm}_{\mu}(x)$ have the propertie

$$\begin{aligned}\widehat{C}J^{L,\pm}_{\mu}(x)\widehat{C}^{-1}&=\pm J^{L,\pm}_{\mu}(x),\\ \widehat{C}J^{H,\mp}_{\mu}(x)\widehat{C}^{-1}&=\mp J^{H,\mp}_{\mu}(x),\end{aligned} \tag{8}$$

which originate from the charge conjunction properties of the scalar, pseudoscalar, axial-vector and vector diquark states,

$$\begin{aligned}\widehat{C}\left[\epsilon^{ijk}q^jC\gamma_5c^k\right]\widehat{C}^{-1}&=\epsilon^{ijk}\bar{q}^j\gamma_5C\bar{c}^k,\\ \widehat{C}\left[\epsilon^{ijk}q^jCc^k\right]\widehat{C}^{-1}&=\epsilon^{ijk}\bar{q}^jC\bar{c}^k,\\ \widehat{C}\left[\epsilon^{ijk}q^jC\gamma_\mu c^k\right]\widehat{C}^{-1}&=\epsilon^{ijk}\bar{q}^j\gamma_\mu C\bar{c}^k,\\ \widehat{C}\left[\epsilon^{ijk}q^jC\gamma_\mu\gamma_5c^k\right]\widehat{C}^{-1}&=-\epsilon^{ijk}\bar{q}^j\gamma_5\gamma_\mu C\bar{c}^k,\end{aligned} \tag{9}$$

where $q=u,d,s$. Naively, we expect that the currents $J^{H,\pm}_{\mu}(x)$ couple to the hidden-charm tetraquark states with higher masses than that of the currents $J^{L,\pm}_{\mu}(x)$, as the scalar $(C\gamma_5)$ and axial-vector $(C\gamma_\mu)$ diquark states are much stable compared to the corresponding pseudoscalar (C) and vector $(C\gamma_\mu\gamma_5)$ diquark states [30–32]. In this article, we study the $J^{PC}=1^{+-}$ diquark–antidiquark type hidden-charm tetraquark states as a byproduct.

On the phenomenological side, we insert a complete set of intermediate hadronic states with the same quantum numbers as the current operators $J^{L/H,\pm}_{\mu}(x)$ into the correlation functions $\Pi^{\pm}_{\mu\nu}(p)$ to obtain the hadronic representation [40–42]. After isolating the ground state hidden-charm tetraquark states $X_{L/H,\pm}$ and $X'_{L/H,\pm}$ contributions from the pole terms, we get the following result:

$$\begin{aligned}\Pi^{\pm}_{\mu\nu}(p)=&\frac{\lambda^2_{X_{L/H,\pm}}}{M^2_{X_{L/H,\pm}}-p^2}\left(-g_{\mu\nu}+\frac{p_\mu p_\nu}{p^2}\right)\\&+\frac{\widetilde{\lambda}^2_{X_{L/H,\pm}}}{\widetilde{M}^2_{X_{L/H,\pm}}-p^2}\,p_\mu p_\nu+\cdots,\\=&\,\Pi_{L/H,\pm}(p)\left(-g_{\mu\nu}+\frac{p_\mu p_\nu}{p^2}\right)\\&+\widetilde{\Pi}_{L/H,\pm}(p)\,p_\mu p_\nu,\end{aligned} \tag{10}$$

where the pole residues (or coupling constants) $\lambda_{X_{L/H,\pm}}$ and $\widetilde{\lambda}_{X_{L/H,\pm}}$ are defined by

$$\begin{aligned}\langle 0|J^{L/H,\pm}_{\mu}(0)|X_{L/H,\pm}(p)\rangle&=\lambda_{X_{L/H,\pm}}\,\varepsilon_\mu,\\ \langle 0|J^{L/H,\pm}_{\mu}(0)|X'_{L/H,\pm}(p)\rangle&=\widetilde{\lambda}_{X_{L/H,\pm}}\,p_\mu,\end{aligned} \tag{11}$$

the ε_μ are the polarization vectors of the axial-vector tetraquark states $X_{L/H,\pm}$. In this article, we choose the tensor structure $-g_{\mu\nu}+\frac{p_\mu p_\nu}{p^2}$ for analysis, the pseudoscalar tetraquark states $X'_{L/H,\pm}$ have no contaminations.

In the following, we briefly outline the operator product expansion for the correlation functions $\Pi^{\pm}_{\mu\nu}(p)$ in perturbative QCD. We contract the quark fields in the correlation functions $\Pi^{\pm}_{\mu\nu}(p)$ with the Wick theorem first, and we obtain the results

$$\Pi^{L,\pm}_{\mu\nu}(p) = -\frac{i\epsilon^{ijk}\epsilon^{imn}\epsilon^{i'j'k'}\epsilon^{i'm'n'}}{2}\int \mathrm{d}^4x \mathrm{e}^{ip\cdot x} \times \Big\{ \mathrm{Tr}\Big[\gamma_5 C^{kk'}(x)\gamma_5 C S^{jj'T}(x) C\Big] \times \mathrm{Tr}\Big[\gamma_\nu C^{n'n}(-x)\gamma_\mu C S^{m'mT}(-x) C\Big] + \mathrm{Tr}\Big[\gamma_\mu C^{kk'}(x)\gamma_\nu C S^{jj'T}(x) C\Big] \times \mathrm{Tr}\Big[\gamma_5 C^{n'n}(-x)\gamma_5 C S^{m'mT}(-x) C\Big] - t\,\mathrm{Tr}\Big[\gamma_\mu C^{kk'}(x)\gamma_5 C S^{jj'T}(x) C\Big] \times \mathrm{Tr}\Big[\gamma_\nu C^{n'n}(-x)\gamma_5 C S^{m'mT}(-x) C\Big] - t\,\mathrm{Tr}\Big[\gamma_5 C^{kk'}(x)\gamma_\nu C S^{jj'T}(x) C\Big] \times \mathrm{Tr}\Big[\gamma_5 C^{n'n}(-x)\gamma_\mu C S^{m'mT}(-x) C\Big]\Big\}, \quad (12)$$

$$\Pi^{H,\mp}_{\mu\nu}(p) = -\frac{i\epsilon^{ijk}\epsilon^{imn}\epsilon^{i'j'k'}\epsilon^{i'm'n'}}{2}\int \mathrm{d}^4x \mathrm{e}^{ip\cdot x} \times \Big\{ \mathrm{Tr}\Big[\gamma_5 \overline{C}^{kk'}(x)\gamma_5 C S^{jj'T}(x) C\Big] \times \mathrm{Tr}\Big[\gamma_\nu \overline{C}^{n'n}(-x)\gamma_\mu C S^{m'mT}(-x) C\Big] + \mathrm{Tr}\Big[\gamma_\mu \overline{C}^{kk'}(x)\gamma_\nu C S^{jj'T}(x) C\Big] \times \mathrm{Tr}\Big[\gamma_5 \overline{C}^{n'n}(-x)\gamma_5 C S^{m'mT}(-x) C\Big] + t\,\mathrm{Tr}\Big[\gamma_\mu \overline{C}^{kk'}(x)\gamma_5 C S^{jj'T}(x) C\Big] \times \mathrm{Tr}\Big[\gamma_\nu \overline{C}^{n'n}(-x)\gamma_5 C S^{m'mT}(-x) C\Big] + t\,\mathrm{Tr}\Big[\gamma_5 \overline{C}^{kk'}(x)\gamma_\nu C S^{jj'T}(x) C\Big] \times \mathrm{Tr}\Big[\gamma_5 \overline{C}^{n'n}(-x)\gamma_\mu C S^{m'mT}(-x) C\Big]\Big\}, \quad (13)$$

where $t = \pm$, $\overline{C}_{ij}(x) = \gamma_5 C_{ij}(x)\gamma_5$, the $S_{ij}(x)$ and $C_{ij}(x)$ are the full s and c quark propagators, respectively [42,43],

$$S^{ij}(x) = \frac{i\delta_{ij}\not{x}}{2\pi^2x^4} - \frac{\delta_{ij}m_s}{4\pi^2x^2} - \frac{\delta_{ij}\langle\bar{s}s\rangle}{12} + \frac{i\delta_{ij}\not{x}m_s\langle\bar{s}s\rangle}{48} - \frac{\delta_{ij}x^2\langle\bar{s}g_s\sigma Gs\rangle}{192} + \frac{i\delta_{ij}x^2\not{x}m_s\langle\bar{s}g_s\sigma Gs\rangle}{1152} - \frac{ig_sG^a_{\alpha\beta}t^a_{ij}(\not{x}\sigma^{\alpha\beta} + \sigma^{\alpha\beta}\not{x})}{32\pi^2x^2} - \frac{i\delta_{ij}x^2\not{x}g_s^2\langle\bar{s}s\rangle^2}{7776} - \frac{\delta_{ij}x^4\langle\bar{s}s\rangle\langle g_s^2GG\rangle}{27648} - \frac{1}{8}\langle\bar{s}_j\sigma^{\mu\nu}s_i\rangle\sigma_{\mu\nu} - \frac{1}{4}\langle\bar{s}_j\gamma^\mu s_i\rangle\gamma_\mu + \cdots, \quad (14)$$

$$C_{ij}(x) = \frac{i}{(2\pi)^4}\int \mathrm{d}^4k \mathrm{e}^{-ik\cdot x}\Big\{\frac{\delta_{ij}}{\not{k}-m_c} - \frac{g_sG^n_{\alpha\beta}t^n_{ij}}{4}\frac{\sigma^{\alpha\beta}(\not{k}+m_c)+(\not{k}+m_c)\sigma^{\alpha\beta}}{(k^2-m_c^2)^2} + \frac{g_sD_\alpha G^n_{\beta\lambda}t^n_{ij}(f^{\lambda\beta\alpha}+f^{\lambda\alpha\beta})}{3(k^2-m_c^2)^4} - \frac{g_s^2(t^at^b)_{ij}G^a_{\alpha\beta}G^b_{\mu\nu}(f^{\alpha\beta\mu\nu}+f^{\alpha\mu\beta\nu}+f^{\alpha\mu\nu\beta})}{4(k^2-m_c^2)^5} + \cdots\Big\}, \quad (15)$$

$$f^{\lambda\alpha\beta} = (\not{k}+m_c)\gamma^\lambda(\not{k}+m_c)\gamma^\alpha(\not{k}+m_c)\gamma^\beta(\not{k}+m_c),$$
$$f^{\alpha\beta\mu\nu} = (\not{k}+m_c)\gamma^\alpha(\not{k}+m_c)\gamma^\beta(\not{k}+m_c)\gamma^\mu(\not{k}+m_c)\gamma^\nu(\not{k}+m_c), \quad (16)$$

and $t^n = \frac{\lambda^n}{2}$, the λ^n is the Gell-Mann matrix, $D_\alpha = \partial_\alpha - ig_sG^n_\alpha t^n$ [42]; we add the superscripts L and H to denote which interpolating current is used. Then we compute the integrals both in the coordinate space and in the momentum space, and we obtain the correlation functions $\Pi^{L/H,\pm}_{\mu\nu}(p)$ at the quark level. The calculations are straightforward but tedious. Once the analytical expressions of the correlation functions $\Pi_{L/H,\pm}(p)$ are gotten, we can obtain the QCD spectral densities $\rho_{L/H,\pm}(s)$ through the dispersion relation. In Eq. (14), we retain the terms $\langle\bar{s}_j\sigma_{\mu\nu}s_i\rangle$ and $\langle\bar{s}_j\gamma_\mu s_i\rangle$ originate from the Fierz re-ordering of the $\langle s_i\bar{s}_j\rangle$ to absorb the gluons emitted from the heavy quark lines to form $\langle\bar{s}_jg_sG^a_{\alpha\beta}t^a_{mn}\sigma_{\mu\nu}s_i\rangle$ and $\langle\bar{s}_j\gamma_\mu s_ig_sD_\nu G^a_{\alpha\beta}t^a_{mn}\rangle$ to extract the mixed condensate and four-quark condensates $\langle\bar{s}g_s\sigma Gs\rangle$ and $g_s^2\langle\bar{s}s\rangle^2$, respectively.

Once the explicit expressions of the QCD spectral densities $\rho_{L/H,\pm}(s)$ are obtained, we take the quark–hadron duality below the continuum thresholds s_0 and perform a Borel transform with respect to the variable $P^2 = -p^2$ to obtain the following four QCD sum rules:

$$\lambda^2_{X_{L,\pm}}\exp\left(-\frac{M^2_{X_{L,\pm}}}{T^2}\right) = \int_{4m_c^2}^{s_0}\mathrm{d}s\,\rho_{L,\pm}(s)\exp\left(-\frac{s}{T^2}\right), \quad (17)$$

$$\lambda^2_{X_{H,\mp}}\exp\left(-\frac{M^2_{X_{H,\mp}}}{T^2}\right) = \int_{4m_c^2}^{s_0}\mathrm{d}s\,\rho_{H,\pm}(s)\exp\left(-\frac{s}{T^2}\right), \quad (18)$$

where

$$\rho_{L,t}(s) = \rho_0(s)+\rho_3(s)+\rho_4(s)+\rho_5(s)+\rho_6(s)+\rho_7(s)+\rho_8(s)+\rho_{10}(s), \quad (19)$$
$$\rho_{H,t}(s) = \rho_{L,t}(s)\,|_{m_c\to-m_c,t\to-t}, \quad (20)$$

$$\rho_0(s) = \frac{1}{3072\pi^6}\int_{y_i}^{y_f}\mathrm{d}y\int_{z_i}^{1-y}\mathrm{d}z\,yz(1-y-z)^3\left(s-\overline{m}_c^2\right)^2\times\left(35s^2-26s\overline{m}_c^2+3\overline{m}_c^4\right) - \frac{3m_sm_c}{512\pi^6}\int_{y_i}^{y_f}\mathrm{d}y\int_{z_i}^{1-y}dz\,(y+z)(1-y-z)^2\times\left(s-\overline{m}_c^2\right)^2\left(3s-\overline{m}_c^2\right), \quad (21)$$

$$\rho_3(s) = -\frac{m_c\langle\bar{s}s\rangle}{64\pi^4}\int_{y_i}^{y_f}\mathrm{d}y\int_{z_i}^{1-y}\mathrm{d}z\,(y+z)(1-y-z)\times\left(s-\overline{m}_c^2\right)\left(7s-3\overline{m}_c^2\right) -\frac{m_s\langle\bar{s}s\rangle}{32\pi^4}\int_{y_i}^{y_f}\mathrm{d}y\int_{z_i}^{1-y}\mathrm{d}z\,yz\,(1-y-z)\times\left(15s^2-16s\overline{m}_c^2+3\overline{m}_c^4\right) +\frac{m_s m_c^2\langle\bar{s}s\rangle}{8\pi^4}\int_{y_i}^{y_f}\mathrm{d}y\int_{z_i}^{1-y}\mathrm{d}z\left(s-\overline{m}_c^2\right), \quad (22)$$

$$\rho_4(s) = -\frac{m_c^2}{2304\pi^4}\left\langle\frac{\alpha_s GG}{\pi}\right\rangle\int_{y_i}^{y_f}\mathrm{d}y\int_{z_i}^{1-y}\mathrm{d}z\left(\frac{z}{y^2}+\frac{y}{z^2}\right)\times(1-y-z)^3\left\{8s-3\overline{m}_c^2+s^2\,\delta\left(s-\overline{m}_c^2\right)\right\} +\frac{1}{1536\pi^4}\left\langle\frac{\alpha_s GG}{\pi}\right\rangle\int_{y_i}^{y_f}\mathrm{d}y\int_{z_i}^{1-y}\mathrm{d}z(y+z)\times(1-y-z)^2\,s\,(5s-4\overline{m}_c^2) -\frac{tm_c^2}{1152\pi^4}\left\langle\frac{\alpha_s GG}{\pi}\right\rangle\int_{y_i}^{y_f}\mathrm{d}y\int_{z_i}^{1-y}\mathrm{d}z\left(s-\overline{m}_c^2\right)\times\left\{1-\left(\frac{1}{y}+\frac{1}{z}\right)(1-y-z) +\frac{(1-y-z)^2}{2yz}-\frac{1-y-z}{2}+\left(\frac{1}{y}+\frac{1}{z}\right)\times\frac{(1-y-z)^2}{4}-\frac{(1-y-z)^3}{12yz}\right\} +\frac{m_s m_c^3}{512\pi^4}\left\langle\frac{\alpha_s GG}{\pi}\right\rangle\int_{y_i}^{y_f}\mathrm{d}y\int_{z_i}^{1-y}\mathrm{d}z\left(\frac{1}{z^3}+\frac{1}{y^3}\right)\times(y+z)(1-y-z)^2\left\{1+\frac{2}{3}\,s\,\delta\left(s-\overline{m}_c^2\right)\right\} -\frac{m_s m_c}{512\pi^4}\left\langle\frac{\alpha_s GG}{\pi}\right\rangle\int_{y_i}^{y_f}\mathrm{d}y\int_{z_i}^{1-y}\mathrm{d}z\left(\frac{y}{z^2}+\frac{z}{y^2}\right)\times(1-y-z)^2\left(5s-3\overline{m}_c^2\right) -\frac{m_s m_c}{768\pi^4}\left\langle\frac{\alpha_s GG}{\pi}\right\rangle\int_{y_i}^{y_f}\mathrm{d}y\int_{z_i}^{1-y}\mathrm{d}z\times(1-y-z)\left(5s-3\overline{m}_c^2\right) -\frac{tm_s m_c}{1152\pi^4}\left\langle\frac{\alpha_s GG}{\pi}\right\rangle\int_{y_i}^{y_f}\mathrm{d}y\int_{z_i}^{1-y}\mathrm{d}z\times(1-y-z)\left(5s-3\overline{m}_c^2\right) +\frac{tm_s m_c}{4608\pi^4}\left\langle\frac{\alpha_s GG}{\pi}\right\rangle\int_{y_i}^{y_f}\mathrm{d}y\int_{z_i}^{1-y}\mathrm{d}z\left(\frac{1}{y}+\frac{1}{z}\right)\times(1-y-z)^2\left(5s-3\overline{m}_c^2\right), \quad (23)$$

$$\rho_5(s) = \frac{m_c\langle\bar{s}g_s\sigma Gs\rangle}{128\pi^4}\int_{y_i}^{y_f}\mathrm{d}y\int_{z_i}^{1-y}\mathrm{d}z(y+z)\left(5s-3\overline{m}_c^2\right) -\frac{m_c\langle\bar{s}g_s\sigma Gs\rangle}{128\pi^4}\int_{y_i}^{y_f}\mathrm{d}y\int_{z_i}^{1-y}\mathrm{d}z\left(\frac{y}{z}+\frac{z}{y}\right)(1-y-z)\times\left(2s-\overline{m}_c^2\right) -\frac{tm_c\langle\bar{s}g_s\sigma Gs\rangle}{1152\pi^4}\int_{y_i}^{y_f}\mathrm{d}y\int_{z_i}^{1-y}\mathrm{d}z\left(\frac{y}{z}+\frac{z}{y}\right)(1-y-z)\times\left(5s-3\overline{m}_c^2\right)-\frac{m_s m_c^2\langle\bar{s}g_s\sigma Gs\rangle}{32\pi^4}\int_{y_i}^{y_f}\mathrm{d}y +\frac{m_s\langle\bar{s}g_s\sigma Gs\rangle}{96\pi^4}\int_{y_i}^{y_f}dy\int_{z_i}^{1-y}\mathrm{d}z\,yz\left\{8s-3\overline{m}_c^2+s^2\times\delta\left(s-\overline{m}_c^2\right)\right\} +\frac{m_s m_c^2\langle\bar{s}g_s\sigma Gs\rangle}{128\pi^4}\int_{y_i}^{y_f}\mathrm{d}y\int_{z_i}^{1-y}\mathrm{d}z\left(\frac{1}{y}+\frac{1}{z}\right) +\frac{tm_s\langle\bar{s}g_s\sigma Gs\rangle}{1152\pi^4}\int_{y_i}^{y_f}\mathrm{d}y\int_{z_i}^{1-y}\mathrm{d}z\,(y+z)\left(5s-3\overline{m}_c^2\right), \quad (24)$$

$$\rho_6(s) = \frac{m_c^2\langle\bar{s}s\rangle^2}{12\pi^2}\int_{y_i}^{y_f}\mathrm{d}y+\frac{g_s^2\langle\bar{s}s\rangle^2}{648\pi^4}\int_{y_i}^{y_f}\mathrm{d}y\int_{z_i}^{1-y}\mathrm{d}z\,yz\times\left\{8s-3\overline{m}_c^2+s^2\,\delta\left(s-\overline{m}_c^2\right)\right\} -\frac{g_s^2\langle\bar{s}s\rangle^2}{2592\pi^4}\int_{y_i}^{y_f}\mathrm{d}y\int_{z_i}^{1-y}\mathrm{d}z(1-y-z)\times\left\{\left(\frac{z}{y}+\frac{y}{z}\right)3\left(7s-4\overline{m}_c^2\right) +\left(\frac{z}{y^2}+\frac{y}{z^2}\right)m_c^2\left[7+5s\,\delta\left(s-\overline{m}_c^2\right)\right] -(y+z)\left(4s-3\overline{m}_c^2\right)\right\} -\frac{g_s^2\langle\bar{s}s\rangle^2}{3888\pi^4}\int_{y_i}^{y_f}\mathrm{d}y\int_{z_i}^{1-y}\mathrm{d}z(1-y-z)\times\left\{\left(\frac{z}{y}+\frac{y}{z}\right)3\left(2s-\overline{m}_c^2\right) +\left(\frac{z}{y^2}+\frac{y}{z^2}\right)m_c^2\left[1+s\,\delta\left(s-\overline{m}_c^2\right)\right] +(y+z)2\left[8s-3\overline{m}_c^2+s^2\,\delta\left(s-\overline{m}_c^2\right)\right]\right\} -\frac{m_s m_c g_s^2\langle\bar{s}s\rangle^2}{864\pi^4}\int_{y_i}^{y_f}\mathrm{d}y\left\{1+\frac{2}{3}\,s\,\delta\left(s-\widetilde{m}_c^2\right)\right\} +\frac{m_s m_c g_s^2\langle\bar{s}s\rangle^2}{2592\pi^4}\int_{y_i}^{y_f}\mathrm{d}y\int_{z_i}^{1-y}\mathrm{d}z\left\{\frac{9-y}{y} +\frac{9-z}{z}+5m_c^2\left(\frac{1}{y^2}+\frac{1}{z^2}\right)\delta\left(s-\overline{m}_c^2\right)\right\} +\frac{m_s m_c g_s^2\langle\bar{s}s\rangle^2}{864\pi^4}\int_{y_i}^{y_f}\mathrm{d}y\int_{z_i}^{1-y}\mathrm{d}z\left(\frac{y}{z}+\frac{z}{y}\right)\times\left\{1+\frac{2}{3}\,s\,\delta\left(s-\overline{m}_c^2\right)\right\}$$

$$+\frac{m_s m_c\langle\bar{s}s\rangle^2}{16\pi^2}\int_{y_i}^{y_f}\mathrm{d}y\left\{1+\frac{2}{3}s\,\delta\left(s-\widetilde{m}_c^2\right)\right\}, \tag{25}$$

$$\begin{aligned}
\rho_7(s) = {} & \frac{m_c^3\langle\bar{s}s\rangle}{576\pi^2}\left\langle\frac{\alpha_s GG}{\pi}\right\rangle\int_{y_i}^{y_f}\mathrm{d}y\int_{z_i}^{1-y}\mathrm{d}z\left(\frac{1}{z^3}+\frac{1}{y^3}\right)(y+z)\\
&\times(1-y-z)\left(1+\frac{2s}{T^2}\right)\delta\left(s-\overline{m}_c^2\right)\\
&-\frac{m_c\langle\bar{s}s\rangle}{64\pi^2}\left\langle\frac{\alpha_s GG}{\pi}\right\rangle\int_{y_i}^{y_f}\mathrm{d}y\int_{z_i}^{1-y}\mathrm{d}z\left(\frac{y}{z^2}+\frac{z}{y^2}\right)\\
&\times(1-y-z)\left\{1+\frac{2s}{3}\delta\left(s-\overline{m}_c^2\right)\right\}\\
&-\frac{m_c\langle\bar{s}s\rangle}{192\pi^2}\left\langle\frac{\alpha_s GG}{\pi}\right\rangle\int_{y_i}^{y_f}\mathrm{d}y\int_{z_i}^{1-y}\mathrm{d}z\\
&\times\left\{1+\frac{2s}{3}\delta\left(s-\overline{m}_c^2\right)\right\}\\
&-\frac{tm_c\langle\bar{s}s\rangle}{288\pi^2}\left\langle\frac{\alpha_s GG}{\pi}\right\rangle\int_{y_i}^{y_f}\mathrm{d}y\int_{z_i}^{1-y}\mathrm{d}z\left\{1\right.\\
&\left.-\left(\frac{1}{y}+\frac{1}{z}\right)\frac{1-y-z}{2}\right\}\left\{1+\frac{2s}{3}\delta\left(s-\overline{m}_c^2\right)\right\}\\
&-\frac{m_c\langle\bar{s}s\rangle}{384\pi^2}\left\langle\frac{\alpha_s GG}{\pi}\right\rangle\int_{y_i}^{y_f}\mathrm{d}y\left\{1+\frac{2s}{3}\delta\left(s-\widetilde{m}_c^2\right)\right\}\\
&+\frac{m_s m_c^2\langle\bar{s}s\rangle}{288\pi^2T^2}\left\langle\frac{\alpha_s GG}{\pi}\right\rangle\int_{y_i}^{y_f}\mathrm{d}y\int_{z_i}^{1-y}\mathrm{d}z\left(\frac{y}{z^2}+\frac{z}{y^2}\right)\\
&\times(1-y-z)\left(s+\frac{s^2}{T^2}\right)\delta\left(s-\overline{m}_c^2\right)\\
&-\frac{m_s m_c^4\langle\bar{s}s\rangle}{144\pi^2T^2}\left\langle\frac{\alpha_s GG}{\pi}\right\rangle\int_{y_i}^{y_f}\mathrm{d}y\int_{z_i}^{1-y}\mathrm{d}z\\
&\times\left(\frac{1}{z^3}+\frac{1}{y^3}\right)\delta\left(s-\overline{m}_c^2\right)\\
&+\frac{m_s m_c^2\langle\bar{s}s\rangle}{48\pi^2}\left\langle\frac{\alpha_s GG}{\pi}\right\rangle\int_{y_i}^{y_f}\mathrm{d}y\int_{z_i}^{1-y}\mathrm{d}z\\
&\times\left(\frac{1}{z^2}+\frac{1}{y^2}\right)\delta\left(s-\overline{m}_c^2\right)\\
&-\frac{m_s\langle\bar{s}s\rangle}{576\pi^2}\left\langle\frac{\alpha_s GG}{\pi}\right\rangle\int_{y_i}^{y_f}\mathrm{d}y\int_{z_i}^{1-y}\mathrm{d}z\\
&\times(y+z)\left(1+\frac{s}{2T^2}\right)\delta\left(s-\overline{m}_c^2\right)\\
&+\frac{tm_s m_c^2\langle\bar{s}s\rangle}{3456\pi^2}\left\langle\frac{\alpha_s GG}{\pi}\right\rangle\int_{y_i}^{y_f}\mathrm{d}y\int_{z_i}^{1-y}\mathrm{d}z\\
&\times\frac{2+3y+3z}{yz}\delta\left(s-\overline{m}_c^2\right)\\
&-\frac{tm_s m_c^2\langle\bar{s}s\rangle}{1728\pi^2}\left\langle\frac{\alpha_s GG}{\pi}\right\rangle\int_{y_i}^{y_f}\mathrm{d}y\\
&\times\left(\frac{1}{y}+\frac{1}{1-y}\right)\delta\left(s-\widetilde{m}_c^2\right)\\
&-\frac{tm_s\langle\bar{s}s\rangle}{288\pi^2}\left\langle\frac{\alpha_s GG}{\pi}\right\rangle\int_{y_i}^{y_f}\mathrm{d}y\int_{z_i}^{1-y}\mathrm{d}z\\
&\times\left\{1+\frac{2}{3}s\,\delta\left(s-\overline{m}_c^2\right)\right\},
\end{aligned} \tag{26}$$

$$\begin{aligned}
\rho_8(s) = {} & -\frac{m_c^2\langle\bar{s}s\rangle\langle\bar{s}g_s\sigma Gs\rangle}{24\pi^2}\int_0^1\mathrm{d}y\left(1+\frac{s}{T^2}\right)\delta\left(s-\widetilde{m}_c^2\right)\\
&+\frac{m_c^2\langle\bar{s}s\rangle\langle\bar{s}g_s\sigma Gs\rangle}{96\pi^2}\int_0^1\mathrm{d}y\left(\frac{1}{y}+\frac{1}{1-y}\right)\\
&\delta\left(s-\widetilde{m}_c^2\right)\\
&+\frac{t\langle\bar{s}s\rangle\langle\bar{s}g_s\sigma Gs\rangle}{288\pi^2}\int_{y_i}^{y_f}\mathrm{d}y\left\{1+\frac{2s}{3}\delta\left(s-\widetilde{m}_c^2\right)\right\}\\
&-\frac{5m_s m_c\langle\bar{s}s\rangle\langle\bar{s}g_s\sigma Gs\rangle}{288\pi^2}\int_{y_i}^{y_f}\mathrm{d}y\left(1+\frac{3s}{2T^2}+\frac{s^2}{T^4}\right)\\
&\times\delta\left(s-\widetilde{m}_c^2\right)\\
&+\frac{m_s m_c\langle\bar{s}s\rangle\langle\bar{s}g_s\sigma Gs\rangle}{192\pi^2T^2}\int_{y_i}^{y_f}\mathrm{d}y\left(\frac{1-y}{y}+\frac{y}{1-y}\right)s\\
&\times\delta\left(s-\widetilde{m}_c^2\right)\\
&+\frac{tm_s m_c\langle\bar{s}s\rangle\langle\bar{s}g_s\sigma Gs\rangle}{1728\pi^2}\int_{y_i}^{y_f}\mathrm{d}y\left(\frac{1-y}{y}+\frac{y}{1-y}\right)\\
&\left(1+\frac{2s}{T^2}\right)\delta\left(s-\widetilde{m}_c^2\right),
\end{aligned} \tag{27}$$

$$\begin{aligned}
\rho_{10}(s) = {} & \frac{m_c^2\langle\bar{s}g_s\sigma Gs\rangle^2}{192\pi^2T^6}\int_0^1\mathrm{d}y\,s^2\,\delta\left(s-\widetilde{m}_c^2\right)\\
&-\frac{m_c^4\langle\bar{s}s\rangle^2}{216T^4}\left\langle\frac{\alpha_s GG}{\pi}\right\rangle\int_0^1\mathrm{d}y\left\{\frac{1}{y^3}+\frac{1}{(1-y)^3}\right\}\\
&\times\delta\left(s-\widetilde{m}_c^2\right)\\
&+\frac{m_c^2\langle\bar{s}s\rangle^2}{72T^2}\left\langle\frac{\alpha_s GG}{\pi}\right\rangle\int_0^1\mathrm{d}y\left\{\frac{1}{y^2}+\frac{1}{(1-y)^2}\right\}\\
&\times\delta\left(s-\widetilde{m}_c^2\right)\\
&-\frac{t\langle\bar{s}s\rangle^2}{1296}\left\langle\frac{\alpha_s GG}{\pi}\right\rangle\int_0^1\mathrm{d}y\left(1+\frac{2s}{T^2}\right)\delta\left(s-\widetilde{m}_c^2\right)\\
&-\frac{m_c^2\langle\bar{s}g_s\sigma Gs\rangle^2}{384\pi^2T^4}\int_0^1\mathrm{d}y\left(\frac{1}{y}+\frac{1}{1-y}\right)s\,\delta\left(s-\widetilde{m}_c^2\right)\\
&-\frac{t\langle\bar{s}g_s\sigma Gs\rangle^2}{1728\pi^2}\int_0^1\mathrm{d}y\left(1+\frac{3s}{2T^2}+\frac{s^2}{T^4}\right)\delta\left(s-\widetilde{m}_c^2\right)\\
&-\frac{t\langle\bar{s}g_s\sigma Gs\rangle^2}{2304\pi^2}\int_0^1\mathrm{d}y\left(1+\frac{2s}{T^2}\right)\delta\left(s-\widetilde{m}_c^2\right)\\
&+\frac{m_c^2\langle\bar{s}s\rangle^2}{216T^6}\langle\frac{\alpha_s GG}{\pi}\rangle\int_0^1\mathrm{d}y\,s^2\,\delta\left(s-\widetilde{m}_c^2\right)\\
&-\frac{m_s m_c\langle\bar{s}g_s\sigma Gs\rangle^2}{576\pi^2T^2}\int_0^1\mathrm{d}y\left(1+\frac{s}{T^2}+\frac{s^2}{2T^4}-\frac{s^3}{T^6}\right)\\
&\times\delta\left(s-\widetilde{m}_c^2\right)\\
&+\frac{m_s m_c^3\langle\bar{s}s\rangle^2}{288T^4}\left\langle\frac{\alpha_s GG}{\pi}\right\rangle\int_0^1\mathrm{d}y\left[\frac{1}{(1-y)^3}+\frac{1}{y^3}\right]\\
&\times\left(1-\frac{2s}{3T^2}\right)\delta\left(s-\widetilde{m}_c^2\right)\\
&-\frac{m_s m_c\langle\bar{s}s\rangle^2}{288T^2}\left\langle\frac{\alpha_s GG}{\pi}\right\rangle\int_0^1\mathrm{d}y\left[\frac{y}{(1-y)^2}+\frac{1-y}{y^2}\right]
\end{aligned}$$

$$
\begin{aligned}
&\left(1-\frac{2s}{T^2}\right)\delta\left(s-\widetilde{m}_c^2\right)\\
&+\frac{tm_sm_c\langle\bar{s}s\rangle^2}{2592T^2}\left\langle\frac{\alpha_sGG}{\pi}\right\rangle\int_0^1\mathrm{d}y\left(\frac{1}{y}+\frac{1}{1-y}\right)\\
&\times\left(1-\frac{2s}{T^2}\right)\delta\left(s-\widetilde{m}_c^2\right)\\
&+\frac{m_sm_c\langle\bar{s}g_s\sigma Gs\rangle^2}{1152\pi^2T^2}\int_0^1\mathrm{d}y\left(\frac{1-y}{y}+\frac{y}{1-y}\right)\\
&\times\left(1+\frac{s}{T^2}-\frac{s^2}{T^4}\right)\delta\left(s-\widetilde{m}_c^2\right)\\
&+\frac{tm_sm_c\langle\bar{s}g_s\sigma Gs\rangle^2}{10368\pi^2T^2}\int_0^1\mathrm{d}y\left(\frac{1-y}{y}+\frac{y}{1-y}\right)\\
&\times\left(1+\frac{s}{T^2}-\frac{2s^2}{T^4}\right)\delta\left(s-\widetilde{m}_c^2\right)\\
&-\frac{m_sm_c\langle\bar{s}s\rangle^2}{864T^2}\langle\frac{\alpha_sGG}{\pi}\rangle\int_0^1\mathrm{d}y\left(1+\frac{s}{T^2}+\frac{s^2}{2T^4}-\frac{s^3}{T^6}\right)\\
&\times\delta\left(s-\widetilde{m}_c^2\right),
\end{aligned}
\tag{28}
$$

where T^2 is the Borel parameter, $y_f=\frac{1+\sqrt{1-4m_c^2/s}}{2}$, $y_i=\frac{1-\sqrt{1-4m_c^2/s}}{2}$, $z_i=\frac{ym_c^2}{ys-m_c^2}$, $\overline{m}_c^2=\frac{(y+z)m_c^2}{yz}$, $\widetilde{m}_c^2=\frac{m_c^2}{y(1-y)}$, $\int_{y_i}^{y_f}\mathrm{d}y\to\int_0^1\mathrm{d}y$, $\int_{z_i}^{1-y}\mathrm{d}z\to\int_0^{1-y}\mathrm{d}z$ when the δ functions $\delta\left(s-\overline{m}_c^2\right)$ and $\delta\left(s-\widetilde{m}_c^2\right)$ appear.

In this article, we carry out the operator product expansion for the vacuum condensates up to dimension 10, and assume vacuum saturation for the higher dimension vacuum condensates. The vacuum condensates are the vacuum expectations of the operators, we take the truncations $n\leq 10$ and $k\leq 1$ for the operators in a consistent way, and discard the operators of the orders $\mathcal{O}(\alpha_s^k)$ with $k>1$. The terms of the orders $\mathcal{O}(\frac{1}{T^2})$, $\mathcal{O}(\frac{1}{T^4})$, $\mathcal{O}(\frac{1}{T^6})$, $\mathcal{O}(\frac{1}{T^8})$ in the QCD spectral densities manifest themselves at small T^2, and we have to choose a large T^2 to warrant convergence of the operator product expansion and appearance of the Borel platforms. The higher dimension vacuum condensates play an important role in determining the Borel windows, though they play a less important role in the Borel windows.

We differentiate Eqs. (17), (18) with respect to $\frac{1}{T^2}$, then eliminate the pole residues $\lambda_{X_{L,\pm}}$ and $\lambda_{X_{H,\pm}}$, and we obtain the QCD sum rules for the masses of $X_{L,\pm}$ and $X_{H,\pm}$, respectively;

$$
M^2_{X_{L,\pm}}=-\frac{\int_{4m_c^2}^{s_0}\mathrm{d}s\frac{d}{d(1/T^2)}\rho_{L,\pm}(s)\exp\left(-\frac{s}{T^2}\right)}{\int_{4m_c^2}^{s_0}\mathrm{d}s\,\rho_{L,\pm}(s)\exp\left(-\frac{s}{T^2}\right)},
\tag{29}
$$

$$
M^2_{X_{H,\mp}}=-\frac{\int_{4m_c^2}^{s_0}\mathrm{d}s\frac{d}{d(1/T^2)}\rho_{H,\pm}(s)\exp\left(-\frac{s}{T^2}\right)}{\int_{4m_c^2}^{s_0}\mathrm{d}s\,\rho_{H,\pm}(s)\exp\left(-\frac{s}{T^2}\right)}.
\tag{30}
$$

3 Numerical results and discussions

In previous work, we described the hidden-charm and the hidden-bottom four-quark systems $q\bar{q}'Q\bar{Q}$ by a double-well potential [33,36–38]. In the four-quark system $q\bar{q}'Q\bar{Q}$, the heavy quark Q serves as one static well potential and combines with the light quark q to form a heavy diquark $\mathcal{D}_{qQ}$ in color antitriplet, while the heavy antiquark $\bar{Q}$ serves as the other static well potential and combines with the light antiquark $\bar{q}'$ to form a heavy antidiquark $\mathcal{D}_{\bar{q}'\bar{Q}}$ in color triplet. Then the $\mathcal{D}_{qQ}$ and $\mathcal{D}_{\bar{q}'\bar{Q}}$ combine together to form a compact tetraquark state, the two heavy quarks Q and $\bar{Q}$ stabilize the tetraquark state [44].

The doubly heavy tetraquark states are characterized by the effective heavy quark mass $\mathbb{M}_Q$ and the virtuality $V=\sqrt{M^2_{X/Y/Z}-(2\mathbb{M}_Q)^2}$. It is natural to take the energy scale $\mu=V$, the energy-scale formula works well for $X(3872)$, $Z_c(3900)$, $Z_c(4020)$, $Z_c(4025)$, $Z(4430)$, $Y(4660)$, $Z_b(10610)$, and $Z_b(10650)$ in the scenario of tetraquark states [33,36–38,45,46]. In Refs. [33,37], we obtain the effective mass for the diquark–antidiquark type hidden-charm tetraquark states, $\mathbb{M}_c=1.8\,\mathrm{GeV}$. Then we re-checked the numerical calculations and found that there exists a small error involving the mixed condensates. After the small error is corrected, the Borel windows are modified slightly and the numerical results are improved slightly; the conclusions survive. In this article, we choose the updated value $\mathbb{M}_c=1.82\,\mathrm{GeV}$ [46], and we obtain the optimal energy scales $\mu=1.4\,\mathrm{GeV}$ and $2.0\,\mathrm{GeV}$ for the QCD spectral densities of the QCD sum rules for the $Z_c(3900)$ and $X(4140)$, respectively.

Now we choose the input parameters at the QCD side of the QCD sum rules. We take the vacuum condensates to be the standard values $\langle\bar{q}q\rangle=-(0.24\pm0.01\,\mathrm{GeV})^3$, $\langle\bar{s}s\rangle=(0.8\pm0.1)\langle\bar{q}q\rangle$, $\langle\bar{q}g_s\sigma Gq\rangle=m_0^2\langle\bar{q}q\rangle$, $\langle\bar{s}g_s\sigma Gs\rangle=m_0^2\langle\bar{s}s\rangle$, $m_0^2=(0.8\pm0.1)\,\mathrm{GeV}^2$, $\langle\frac{\alpha_sGG}{\pi}\rangle=(0.33\,\mathrm{GeV})^4$ at the energy scale $\mu=1\,\mathrm{GeV}$ [40–42,47], and we take the $\overline{MS}$ masses $m_c(m_c)=(1.275\pm0.025)\,\mathrm{GeV}$ and $m_s(\mu=2\,\mathrm{GeV})=(0.095\pm0.005)\,\mathrm{GeV}$ from the Particle Data Group [27]. Moreover, we take into account the energy-scale dependence of the quark condensates, mixed quark condensates, and $\overline{MS}$ masses from the renormalization group equation [48],

$$
\begin{aligned}
\langle\bar{q}q\rangle(\mu)&=\langle\bar{q}q\rangle(Q)\left[\frac{\alpha_s(Q)}{\alpha_s(\mu)}\right]^{\frac{4}{9}},\\
\langle\bar{s}s\rangle(\mu)&=\langle\bar{s}s\rangle(Q)\left[\frac{\alpha_s(Q)}{\alpha_s(\mu)}\right]^{\frac{4}{9}},\\
\langle\bar{q}g_s\sigma Gq\rangle(\mu)&=\langle\bar{q}g_s\sigma Gq\rangle(Q)\left[\frac{\alpha_s(Q)}{\alpha_s(\mu)}\right]^{\frac{2}{27}},\\
\langle\bar{s}g_s\sigma Gs\rangle(\mu)&=\langle\bar{s}g_s\sigma Gs\rangle(Q)\left[\frac{\alpha_s(Q)}{\alpha_s(\mu)}\right]^{\frac{2}{27}},
\end{aligned}
\tag{31}
$$

$$m_c(\mu)=m_c(m_c)\left[\frac{\alpha_s(\mu)}{\alpha_s(m_c)}\right]^{\frac{12}{25}},$$
$$m_s(\mu)=m_s(2\text{GeV})\left[\frac{\alpha_s(\mu)}{\alpha_s(2\text{GeV})}\right]^{\frac{4}{9}},$$
$$\alpha_s(\mu)=\frac{1}{b_0 t}\left[1-\frac{b_1}{b_0^2}\frac{\log t}{t}+\frac{b_1^2(\log^2 t-\log t-1)+b_0 b_2}{b_0^4 t^2}\right], \quad (32)$$

where $t=\log\frac{\mu^2}{\Lambda^2}$, $b_0=\frac{33-2n_f}{12\pi}$, $b_1=\frac{153-19n_f}{24\pi^2}$, $b_2=\frac{2857-\frac{5033}{9}n_f+\frac{325}{27}n_f^2}{128\pi^3}$, $\Lambda=213$, 296 and 339 MeV for the flavors $n_f=5$, 4 and 3, respectively [27]. In this article, we take the standard value of the quark condensate $\langle\bar{q}q\rangle$ at the energy scale $\mu=1\,\text{GeV}$ from the Gell-Mann–Oakes–Renner relation [40–42,47–49]. The values of the quark condensates have been updated [50], however, we determine the effective heavy quark masses $\mathbb{M}_Q$ with the standard values [33,36–38,45,46], so we choose the standard values in this article. In our next work, we will redetermine the $\mathbb{M}_Q$ with the updated values, as the updated value $\langle\bar{q}q\rangle(2\text{GeV})=-(274^{+15}_{-17}\,\text{MeV})^3$ differs from the standard value $\langle\bar{q}q\rangle(2\text{GeV})=-(257\pm10\,\text{MeV})^3$ considerably.

In this article, we have neglected the higher-order QCD corrections. Including the higher-order QCD corrections means refitting the effective c-quark mass $\mathbb{M}_c$. According to the energy-scale formula $\mu=\sqrt{M^2_{X/Y/Z}-(2\mathbb{M}_c)^2}$, some uncertainties are introduced by neglecting the higher-order QCD corrections. In this article, we take the leading order approximations just as in the QCD sum rules for $X(3872)$, $Z_c(3900)$, $Y(4660)$, some higher-order effects are embodied in the effective c-quark mass $\mathbb{M}_c$ [33,37].

In Ref. [45], we observed that the $Z_c(3900)$ and $Z(4430)$ can be assigned to the ground state and the first radial excited state of the axial-vector tetraquark states with $J^{PC}=1^{+-}$, respectively, based on the QCD sum rules. We expect the energy gap between the ground state and the first radial excited state of the hidden-charm tetraquark states is about 0.6 GeV according to the mass difference $M_{Z(4430)}-M_{Z_c(3900)}=576\,\text{MeV}$. In this article, we assume $X(4140)=X_{L,+}$, then the threshold parameters can be taken as $\sqrt{s_0}=(4.6\text{–}4.8)\,\text{GeV}$. If we choose the energy scale determined by the empirical energy scale formula, then $\mu=2.0\,\text{GeV}$. In calculations, we observe that it is impossible to reproduce the experimental value $M_{X(4140)}=4146.5\pm4.5^{+4.6}_{-2.8}\,\text{MeV}$.

Now we explore the energy-scale dependence of the predicted mass of $X_{L,+}$. In Fig. 1, we plot the mass with variation of the Borel parameter T^2 and energy scale μ for the threshold parameter $\sqrt{s_0}=4.7\,\text{GeV}$. From the figure, we can see that the masses decrease monotonously with increase of the energy scales. The energy scale $\mu=1.1\,\text{GeV}$ is the optimal energy scale to reproduce the experimental value. If we choose the energy scale $\mu=1.1\,\text{GeV}$ and the threshold parameter $\sqrt{s_0}=(4.6-4.8)\,\text{GeV}$, the ideal Borel parameter is $T^2=(2.5-2.9)\,\text{GeV}^2$, the pole contribution is about $(52-75)\%$, the contributions of the vacuum condensates of dimension 8 and 10 are about $-(9\text{–}16)\%$ and $1\ll\%$, respectively. The two criteria of the QCD sum rules (i.e. pole dominance at the phenomenological side and convergence of the operator product expansion at the QCD side) are both satisfied. After taking into account all uncertainties of the input parameters, we obtain the mass and pole residue,

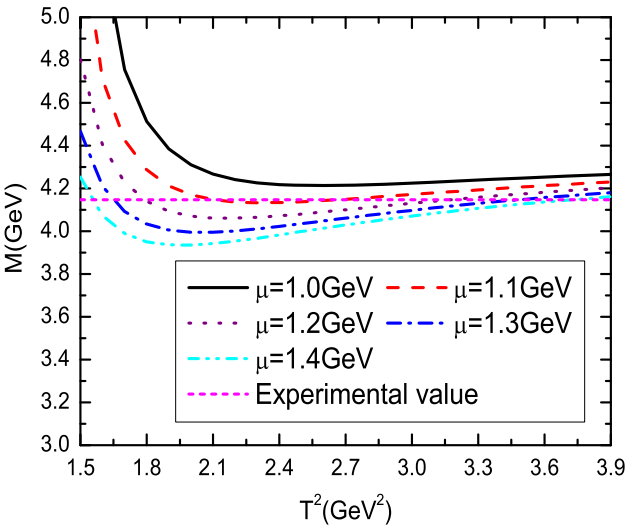

Fig. 1 The masses $M_{X_{L,+}}$ with variations of the Borel parameters T^2 and energy scales μ, where the *horizontal line* denotes the experimental value of the mass $M_{X(4140)}$

$$M_{X_{L,+}}=(4.15\pm0.09)\,\text{GeV},$$
$$\lambda_{X_{L,+}}=(2.10\pm0.30)\times10^{-2}\,\text{GeV}^5, \quad (33)$$

which are shown in Fig. 2 at a large interval of the Borel parameter. The predicted mass $M_{X_{L,+}}=(4.15\pm0.09)\,\text{GeV}$ is in excellent agreement with the experimental value $M_{X(4140)}=4146.5\pm4.5^{+4.6}_{-2.8}\,\text{MeV}$, which favors assigning $X(4140)$ to the 1^{++} diquark–antidiquark type $cs\bar{c}\bar{s}$ tetraquark state. However, we reproduce the experimental value $M_{Z_c(3900)}$ at the energy scale $\mu=1.4\,\text{GeV}$ of the QCD spectral density, while we reproduce the experimental value $M_{X(4140)}$ at the energy scale $\mu=1.1\,\text{GeV}$ of the QCD spectral density. The empirical energy-scale formula can be re-written as

$$M^2_{X/Y/Z}=(2\mathbb{M}_Q)^2+\mu^2, \quad (34)$$

which puts a strong constraint on the masses of the hidden-charm and the hidden-bottom tetraquark states. If the two heavy quarks Q and $\bar{Q}$ serve as a double-well potential and stabilize the tetraquark states, $X(4140)$ should correspond to a larger energy scale than that of the $Z_c(3900)$,

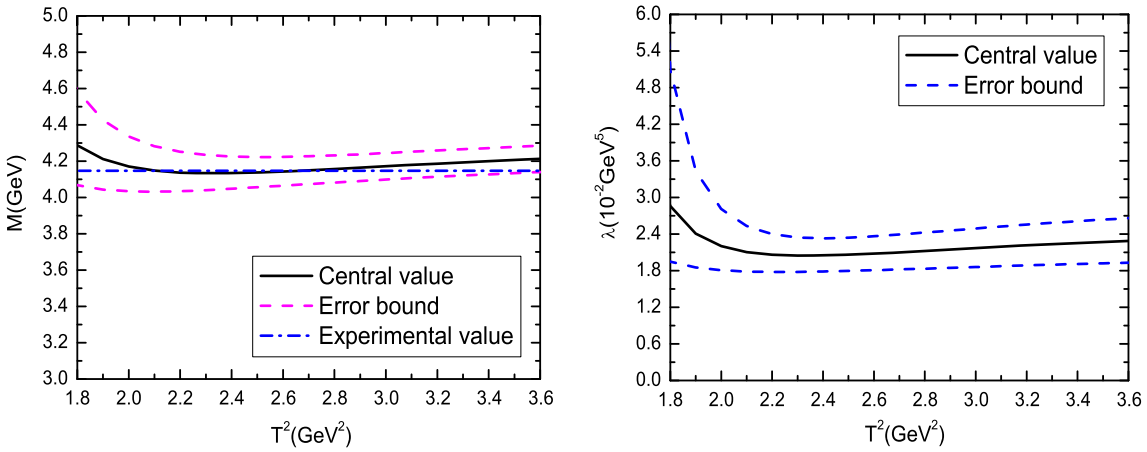

Fig. 2 The mass and pole residue of $X_{L,+}$ with variations of the Borel parameter T^2, where the *horizontal line* denotes the experimental value of the mass $M_{X(4140)}$

i.e. $\mu_{X(4140)} > \mu_{Z_c(3900)}$. Moreover, in previous work, we used the empirical energy-scale formula and reproduced the experimental values of the masses of $X(3872)$, $Z_c(3900)$, $Z_c(4020)$, $Z_c(4025)$, $Z(4430)$, $Y(4660)$, $Z_b(10610)$, and $Z_b(10650)$ in the scenario of tetraquark states [33,36–38,45,46]. It is odd that the QCD spectral density of the QCD sum rules for the $X(4140)$ does not obey the empirical energy-scale formula.

Now we search for the Borel parameters T^2 and continuum threshold parameters s_0 to satisfy the following four criteria:

1. pole dominance at the phenomenological side;
2. convergence of the operator product expansion;
3. appearance of the Borel platforms;
4. satisfying the energy-scale formula,

to obtain the ground state masses of $X_{L,\pm}$ and $X_{H,\pm}$.

The resulting Borel parameters, continuum threshold parameters, energy scales, pole contributions, and contributions of the vacuum condensates of dimension 8 and 10 are shown explicitly in Table 1, where the vacuum condensate contributions D_8 and D_{10} correspond to the central values of the threshold parameters. From the table, we can see that the first two criteria are satisfied.

We take into account all uncertainties of the input parameters, and obtain the values of the ground state masses and pole residues, which are shown explicitly in Table 2 and Figs. 3 and 4. From Tables 1 and 2, we can see that the empirical energy-scale formula is satisfied. From Figs. 3 and 4, we can see that in the Borel windows, the masses and pole residues are rather stable with variations of the Borel parameters. The four criteria are all satisfied, we expect to make reliable predictions. From Fig. 3, we can see that the upper error bound of the theoretical value $M_{X_{L,+}}$ lies below the experimental value $M_{X(4140)}$, the present prediction disfavors assigning $X(4140)$ to be diquark–antidiquark type $cs\bar{c}\bar{s}$ tetraquark state with the $J^{PC} = 1^{++}$. The present predictions of the masses of the axial-vector $cs\bar{c}\bar{s}$ tetraquark states can be confronted to the experimental data in the future.

Now we perform a Fierz re-arrangement to the currents $J_\mu^{L/H,\pm}$ both in the color space and Dirac-spinor space, and we obtain the following results:

Table 2 The masses and pole residues of the axial-vector $cs\bar{c}\bar{s}$ tetraquark states

	M_X (GeV)	$\lambda_X(10^{-2}\ \text{GeV}^5)$
$X_L\ (1^{++})$	3.95 ± 0.09	2.18 ± 0.35
$X_L\ (1^{+-})$	3.97 ± 0.09	2.19 ± 0.35
$X_H\ (1^{+-})$	4.98 ± 0.10	10.7 ± 1.2
$X_H\ (1^{++})$	5.00 ± 0.10	10.9 ± 1.2

Table 1 The Borel parameters, continuum threshold parameters, energy scales, pole contributions, contributions of the vacuum condensates of dimension 8 and 10

	T^2 (GeV^2)	$\sqrt{s_0}$ (GeV)	μ (GeV)	pole	D_8	D_{10}
$X_L\ (1^{++})$	$2.9 - 3.3$	4.5 ± 0.1	1.5	$(40 - 61)\%$	$-(2 - 4)\%$	$\ll 1\%$
$X_L\ (1^{+-})$	$2.9 - 3.3$	4.5 ± 0.1	1.5	$(39 - 61)\%$	$-(4 - 6)\%$	$\ll 1\%$
$X_H\ (1^{+-})$	$4.3 - 4.7$	5.5 ± 0.1	3.4	$(42 - 58)\%$	$< 1\%$	$\ll 1\%$
$X_H\ (1^{++})$	$4.3 - 4.7$	5.5 ± 0.1	3.4	$(41 - 58)\%$	$\ll 1\%$	$\ll 1\%$

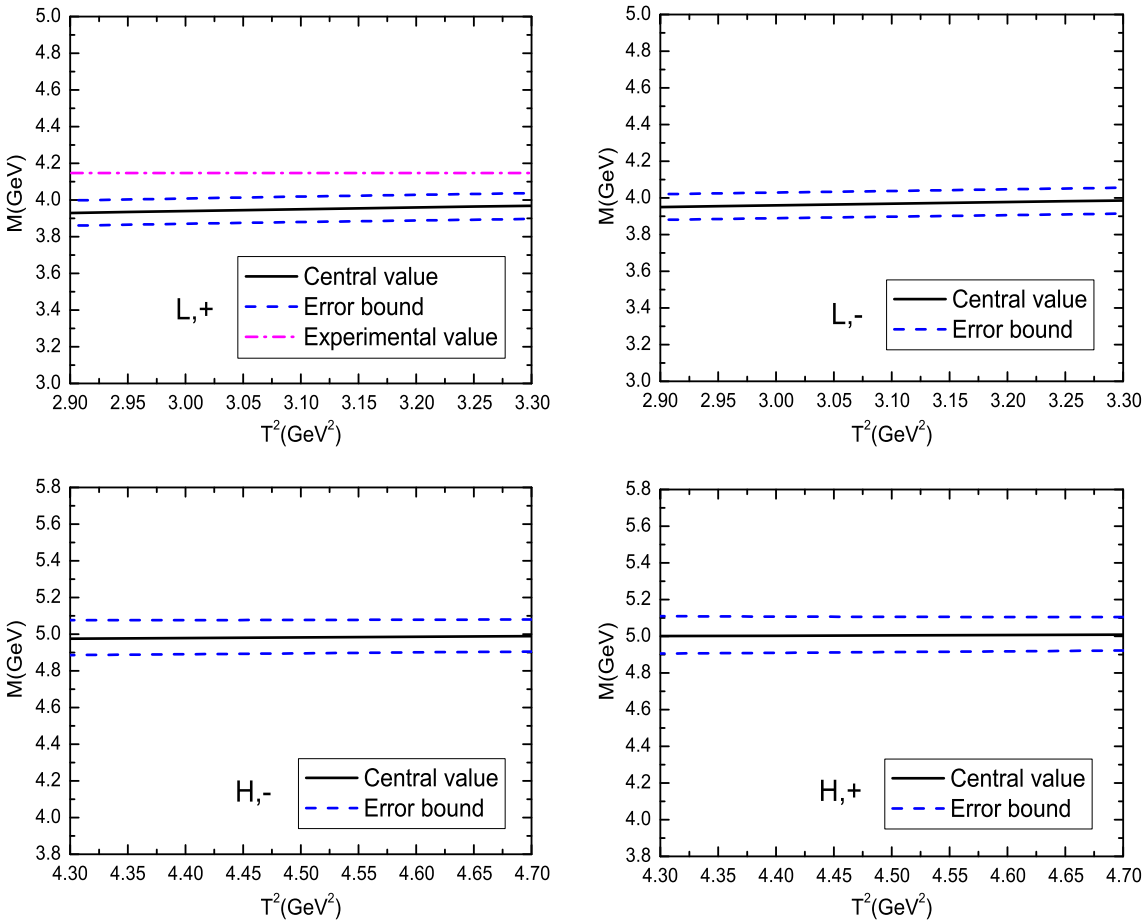

Fig. 3 The masses of the axial-vector $cs\bar{c}\bar{s}$ tetraquark states with variations of the Borel parameters T^2, where the *horizontal line* denotes the experimental value of the mass $M_{X(4140)}$, the positive sign + (negative sign −) denotes the positive charge conjugation (negative charge conjugation)

$$
\begin{aligned}
J^{\mu}_{L,+} = \frac{1}{2\sqrt{2}}\Big\{ & \bar{c}\gamma^{\mu}\gamma_5 c\,\bar{s}s - \bar{c}c\,\bar{s}\gamma^{\mu}\gamma_5 s \\
& -i\bar{c}i\gamma_5 s\,\bar{s}\gamma^{\mu}c + i\bar{c}\gamma^{\mu}s\,\bar{s}i\gamma_5 c \\
& -i\bar{c}\gamma_{\nu}c\,\bar{s}\sigma^{\mu\nu}\gamma_5 s + i\bar{c}\sigma^{\mu\nu}\gamma_5 c\,\bar{s}\gamma_{\nu}s \\
& -i\bar{c}\sigma^{\mu\nu}s\,\bar{s}\gamma_{\nu}\gamma_5 c + i\bar{c}\gamma_{\nu}\gamma_5 s\,\bar{s}\sigma^{\mu\nu}c\Big\}, \qquad (35)
\end{aligned}
$$

$$
\begin{aligned}
J^{\mu}_{L,-} = \frac{1}{2\sqrt{2}}\Big\{ & i\bar{c}i\gamma_5 c\,\bar{s}\gamma^{\mu}s - i\bar{c}\gamma^{\mu}c\,\bar{s}i\gamma_5 s \\
& +\bar{c}s\,\bar{s}\gamma^{\mu}\gamma_5 c - \bar{c}\gamma^{\mu}\gamma_5 s\,\bar{s}c \\
& -i\bar{c}\gamma_{\nu}\gamma_5 c\,\bar{s}\sigma^{\mu\nu}s + i\bar{c}\sigma^{\mu\nu}c\,\bar{s}\gamma_{\nu}\gamma_5 s \\
& -i\bar{c}\sigma^{\mu\nu}\gamma_5 s\,\bar{s}\gamma_{\nu}c + i\bar{c}\gamma_{\nu}s\,\bar{s}\sigma^{\mu\nu}\gamma_5 c\Big\}, \qquad (36)
\end{aligned}
$$

$$
\begin{aligned}
J^{\mu}_{H,-} = \frac{1}{2\sqrt{2}}\Big\{ & -i\bar{c}\gamma^{\mu}c\,\bar{s}i\gamma_5 s - i\bar{c}i\gamma_5 c\,\bar{s}\gamma^{\mu}s \\
& +i\bar{c}i\gamma_5 s\,\bar{s}\gamma^{\mu}c + i\bar{c}\gamma^{\mu}s\,\bar{s}i\gamma_5 c \\
& -i\bar{c}\gamma_{\nu}\gamma_5 c\,\bar{s}\sigma^{\mu\nu}s - i\bar{c}\sigma^{\mu\nu}c\,\bar{s}\gamma_{\nu}\gamma_5 s \\
& +i\bar{c}\sigma^{\mu\nu}s\,\bar{s}\gamma_{\nu}\gamma_5 c + i\bar{c}\gamma_{\nu}\gamma_5 s\,\bar{s}\sigma^{\mu\nu}c\Big\}, \qquad (37)
\end{aligned}
$$

$$
\begin{aligned}
J^{\mu}_{H,+} = \frac{1}{2\sqrt{2}}\Big\{ & \bar{c}c\,\bar{s}\gamma^{\mu}\gamma_5 s + \bar{c}\gamma^{\mu}\gamma_5 c\,\bar{s}s - \bar{c}s\,\bar{s}\gamma^{\mu}\gamma_5 c \\
& -\bar{c}\gamma^{\mu}\gamma_5 s\,\bar{s}c \\
& -i\bar{c}\gamma_{\nu}c\,\bar{s}\sigma^{\mu\nu}\gamma_5 s - i\bar{c}\sigma^{\mu\nu}\gamma_5 c\,\bar{s}\gamma_{\nu}s \\
& +i\bar{c}\sigma^{\mu\nu}\gamma_5 s\,\bar{s}\gamma_{\nu}c + i\bar{c}\gamma_{\nu}s\,\bar{s}\sigma^{\mu\nu}\gamma_5 c\Big\}, \qquad (38)
\end{aligned}
$$

the components such as $\bar{c}i\gamma_5 c\,\bar{s}\gamma^{\mu}s$, $\bar{c}\gamma^{\mu}c\,\bar{s}i\gamma_5 s$, $\bar{c}\gamma_{\nu}c\,\bar{s}\sigma^{\mu\nu}\gamma_5 s$, $\bar{c}\sigma^{\mu\nu}\gamma_5 c\,\bar{s}\gamma_{\nu}s$, etc couple potentially to the molecular states or meson–meson pairs. The physical diquark–antidiquark type tetraquark state can be taken as a special superposition of a series of off-shell molecular states and meson–meson pairs, and embodies the net effects. The decays to its components (meson–meson pairs) are Okubo–Zweig–Iizuka super-allowed, but the re-arrangements in the color space are non-trivial. At the phenomenological side of the QCD sum rules, it is not necessary to include the contributions of the molecular states lying near the physical tetraquark state explicitly, as their effects are already embodied in the physical tetraquark state.

The two-body strong decays

$$
\begin{aligned}
& X_{L,+}(1^{++}) \to J/\psi\phi \to J/\psi\omega \quad (\phi-\omega \text{ mixing}), \\
& X_{L,-}(1^{+-}) \to \eta_c\phi,\ J/\psi\eta, \qquad (39)
\end{aligned}
$$

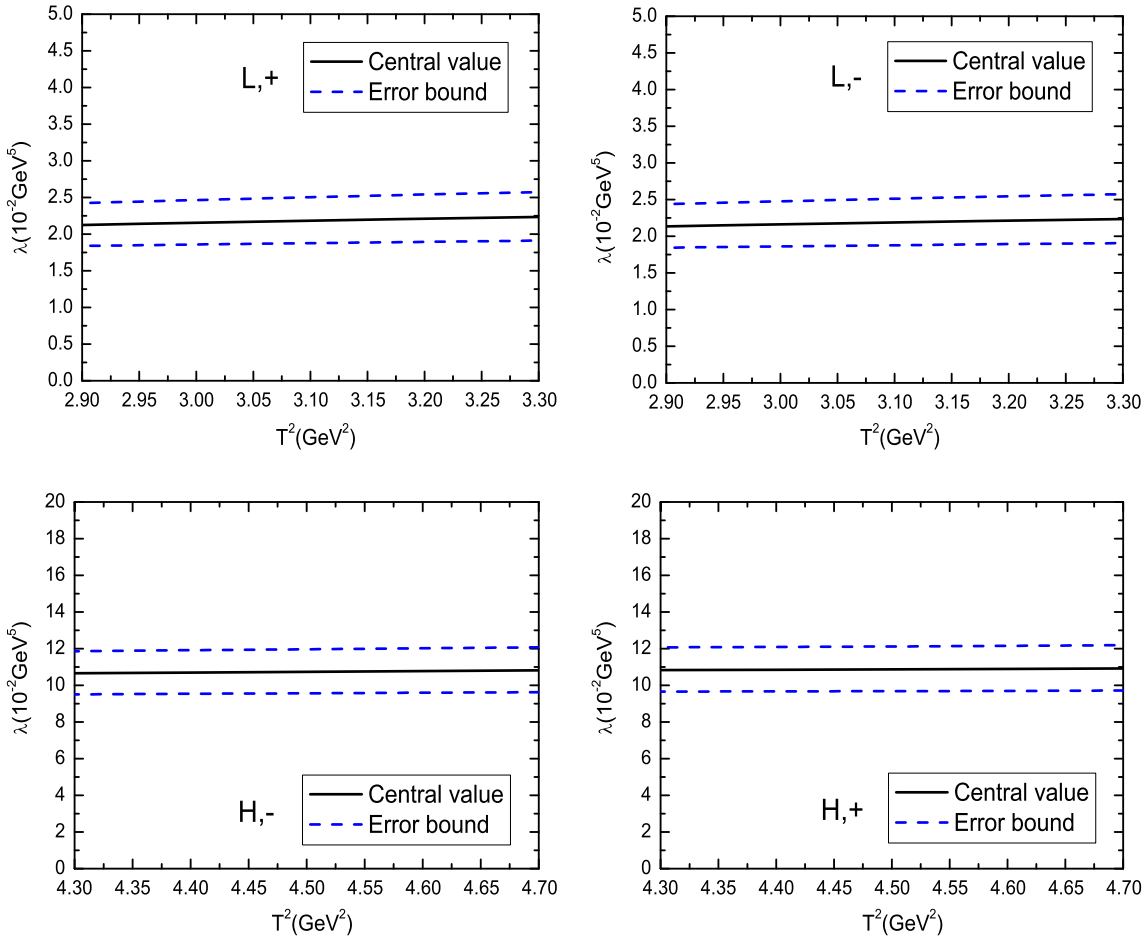

Fig. 4 The pole residues of the axial-vector $cs\bar{c}\bar{s}$ tetraquark states with variations of the Borel parameters T^2, the positive sign + (negative sign −) denotes the positive charge conjugation (negative charge conjugation)

$$
\begin{aligned}
X_{H,-}(1^{+-}) \to\ & \eta_c\phi,\ J/\psi\eta,\ J/\psi\eta',\ D_s^{\pm}D_s^{*\mp},,\\
& \chi_{c1}h_1(1380),\ h_{c1}f_1(1420)\,,\\
X_{H,+}(1^{++}) \to\ & J/\psi\phi,\ \chi_{c0}f_1(1420),\ D_s^{*\pm}D_s^{*\mp},\\
& D_{s0}^{*\pm}(2317)D_{s1}^{*\mp}(2460),
\end{aligned}
\tag{40}
$$

are Okubo–Zweig–Iizuka super-allowed. The decay widths of the $X_{L,+}(1^{++})$ and $X_{L,-}(1^{+-})$ are expected to be small due to the small available phase-spaces, while the decay widths of the $X_{H,+}(1^{++})$ and $X_{H,-}(1^{+-})$ are expected to be large due to the large available phase-spaces.

Now we study the finite width effect on the predicted mass $M_{X_{L,+}}$, which lies in the vicinity of the $M_{X(4140)}$. The current $J_\mu^{L,+}(x)$ couples potentially to the scattering states $J/\psi\omega$, $J/\psi\phi$, $D_s^{*\pm}D_s^{*\mp}$, ..., we take into account the contributions of the intermediate meson loops to the correlation function $\Pi_{L,+}(p^2)$,

$$
\Pi_{L,+}(p^2) = -\frac{\widehat{\lambda}^2_{X_{L,+}}}{p^2-\widehat{M}^2_{X_{L,+}}-\Sigma_{J/\psi\omega}(p)-\Sigma_{J/\psi\phi}(p)+\cdots}+\cdots\,,
\tag{41}
$$

where the $\widehat{\lambda}_{X_{L,+}}$ and $\widehat{M}_{X_{L,+}}$ are bare quantities to absorb the divergences in the self-energies $\Sigma_{J/\psi\omega}(p)$, $\Sigma_{J/\psi\phi}(p)$, ... All the renormalized self-energies contribute a finite imaginary part to modify the dispersion relation,

$$
\Pi_{L,+}(p^2) = -\frac{\lambda^2_{L,+}}{p^2-M^2_{L,+}+i\sqrt{p^2}\Gamma(p^2)}+\cdots\,.
\tag{42}
$$

We can take into account the finite width effect by the following simple replacement of the hadronic spectral density:

$$
\delta\left(s-M^2_{L,+}\right) \to \frac{1}{\pi}\frac{\sqrt{s}\,\Gamma_{L,+}(s)}{\left(s-M^2_{L,+}\right)^2+s\,\Gamma^2_{L,+}(s)}.
\tag{43}
$$

It is easy to obtain the mass,

$$
M^2_{L,+} = \frac{\int_{\Delta^2}^{s^0_{L,+}} \mathrm{d}s\, s\, \frac{1}{\pi}\frac{\sqrt{s}\,\Gamma_{L,+}(s)}{\left(s-M^2_{L,+}\right)^2+s\,\Gamma^2_{L,+}(s)}\,\exp\left(-\frac{s}{T^2}\right)}{\int_{\Delta^2}^{s^0_{L,+}} \mathrm{d}s\, \frac{1}{\pi}\frac{\sqrt{s}\,\Gamma_{L,+}(s)}{\left(s-M^2_{L,+}\right)^2+s\,\Gamma^2_{L,+}(s)}\,\exp\left(-\frac{s}{T^2}\right)},
\tag{44}
$$

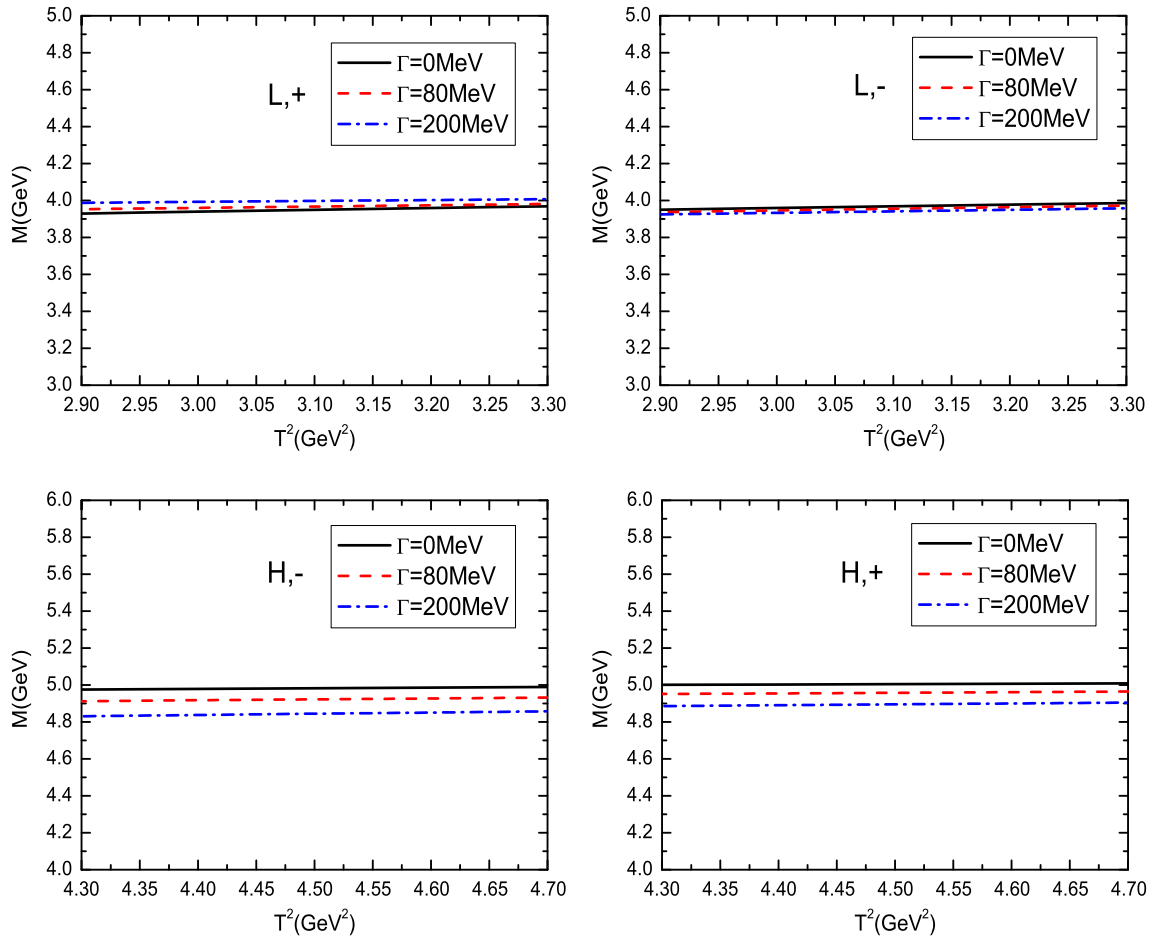

Fig. 5 The masses of the axial-vector $cs\bar{c}\bar{s}$ tetraquark states with variations of the Borel parameters T^2 and the finite widths Γ, where the positive sign $+$ (negative sign $-$) denotes the positive charge conjugation (negative charge conjugation)

where the mass $M_{L,+}$ at the right side of Eq. (44) comes from the QCD sum rules in Eq. (29), $\Gamma_{L,+}(s) = \Gamma_{L,+}$, $\Delta = M_{J/\psi} + M_\omega$. The relevant thresholds are $M_{J/\psi} + M_\phi = 4.11638\,\text{GeV}$ and $M_{J/\psi} + M_\omega = 3.87957\,\text{GeV}$ from the Particle Data Group [27], the decay $X_{L,+} \to J/\psi\phi$ is kinematically forbidden, the decay $X_{L,+} \to J/\psi\omega$ can take place through the ϕ–ω mixing. The width from the LHCb collaboration is $\Gamma_{X(4140)} = 83 \pm 21^{+21}_{-14}\,\text{MeV}$ [24,25], the energy dependence of the small width can be safely neglected. If we assign $X(4140)$ to $X_{L,+}$, then $\Gamma_{L,+} \approx 80\,\text{MeV}$. The numerical result is shown explicitly in Fig. 5. From Fig. 5, we can see that the predicted mass $M_{L,+}$ increases monotonously but slowly with the increase of the finite width $\Gamma_{L,+}$. Now the predicted masses from the QCD sum rules are

$$\begin{aligned} M_{L,+} &= (3.97 \pm 0.09)\,\text{GeV} \quad \text{for} \quad \Gamma_{L,+} = 80\,\text{MeV}, \\ &= (4.00 \pm 0.09)\,\text{GeV} \quad \text{for} \quad \Gamma_{L,+} = 200\,\text{MeV}, \end{aligned} \tag{45}$$

which are still smaller than the experimental value $M_{X(4140)} = 4146.5 \pm 4.5^{+4.6}_{-2.8}\,\text{MeV}$ from the LHCb collaboration [24,25]. Moreover, the decay $X_{L,+} \to J/\psi\phi$ is kinematically forbidden, the total decay width of $X_{L,+}$ cannot exceed 200 MeV. The contributions of the intermediate meson loops to the $X_{L,+}$ cannot impair the predictive ability remarkably.

The contributions of the intermediate meson loops to the $X_{L,-}$, $X_{H,-}$, $X_{H,+}$ can be studied analogously. In calculations, we take the thresholds $\Delta = M_{J/\psi} + M_\eta = 3.64478\,\text{GeV}$ for $X_{L,-}$, $X_{H,-}$ and $\Delta = M_{J/\psi} + M_\omega = 3.87957\,\text{GeV}$ for $X_{H,+}$. Moreover, we take into account of the energy dependence of the finite widths of $X_{H,-}$ and $X_{H,+}$,

$$\begin{aligned} \Gamma_{H,-}(s) &= \Gamma_{H,-}\frac{M^2_{H,-}}{s}\sqrt{\frac{s-(M_{J/\psi}+M_\eta)^2}{M^2_{H,-}-(M_{J/\psi}+M_\eta)^2}}, \\ \Gamma_{H,+}(s) &= \Gamma_{H,+}\frac{M^2_{H,+}}{s}\sqrt{\frac{s-(M_{J/\psi}+M_\omega)^2}{M^2_{H,+}-(M_{J/\psi}+M_\omega)^2}}. \end{aligned} \tag{46}$$

The numerical results are also shown in Fig. 5. From the figure, we can see that the predicted mass $M_{L,-}$ decreases monotonously but very slowly with the increase of the finite

width $\Gamma_{L,-}$, the effect of the finite width $\Gamma_{L,-}$ or the intermediate meson loops can be neglected safely. However, the predicted masses $M_{H,-}$ and $M_{H,+}$ decrease monotonously and remarkably with the increase of the finite widths $\Gamma_{H,-}$ and $\Gamma_{H,+}$, respectively, as they lie far above the corresponding thresholds $\Delta = M_{J/\psi} + M_{\eta} = 3.64478\,\text{GeV}$ and $\Delta = M_{J/\psi} + M_{\omega} = 3.87957\,\text{GeV}$, respectively. For example,

$$\begin{aligned} M_{H,-} &= (4.92 \pm 0.10)\,\text{GeV} \quad \text{for} \quad \Gamma_{H,-} = 80\,\text{MeV}, \\ &= (4.84 \pm 0.10)\,\text{GeV} \quad \text{for} \quad \Gamma_{H,-} = 200\,\text{MeV}, \end{aligned} \tag{47}$$

$$\begin{aligned} M_{H,+} &= (4.96 \pm 0.10)\,\text{GeV} \quad \text{for} \quad \Gamma_{H,+} = 80\,\text{MeV}, \\ &= (4.90 \pm 0.10)\,\text{GeV} \quad \text{for} \quad \Gamma_{H,+} = 200\,\text{MeV}. \end{aligned} \tag{48}$$

The decays $X_{H,-} \to \eta_c\phi$, $J/\psi\eta$, $D_s^{\pm}D_s^{*\mp}$ and $X_{H,+} \to J/\psi\omega$, $J/\psi\phi$, $D_s^{*\pm}D_s^{*\mp}$ can take place easily, the total decay widths may be large and can modify the predicted masses remarkably, the net effects of the intermediate meson loops should be taken into account.

4 Conclusion

In this article, we take $X(4140)$ as the axial-vector $cs\bar{c}\bar{s}$ tetraquark state, construct two diquark–antidiquark type axial-vector currents, calculate the contributions of the vacuum condensates up to dimension 10 in the operator product expansion in a consistent way, use the empirical energy-scale formula to determine the ideal energy scales of the QCD spectral densities, and study the ground state masses and pole residues with the QCD sum rules. The numerical results $M_{X_{L,+}} = 3.95 \pm 0.09\,\text{GeV}$ and $M_{X_{H,+}} = 5.00 \pm 0.10\,\text{GeV}$ disfavor assigning $X(4140)$ to the $J^{PC} = 1^{++}$ diquark–antidiquark type tetraquark states. Moreover, we obtain the masses of the $J^{PC} = 1^{+-}$ diquark–antidiquark type $cs\bar{c}\bar{s}$ tetraquark states as a byproduct. The present predictions of the masses of the axial-vector $cs\bar{c}\bar{s}$ tetraquark states can be confronted to the experimental data in the future.

Acknowledgements This work is supported by National Natural Science Foundation, Grant Numbers 11375063, and Natural Science Foundation of Hebei province, Grant Number A2014502017.

References

1. T. Aaltonen et al., Phys. Rev. Lett. **102**, 242002 (2009)
2. T. Aaltonen et al., arXiv:1101.6058
3. S. Chatrchyan et al., Phys. Lett. B **734**, 261 (2014)
4. V.M. Abazov, Phys. Rev. D **89**, 012004 (2014)
5. X. Liu, S.L. Zhu, Phys. Rev. D **80**, 017502 (2009)
6. T. Branz, T. Gutsche, V.E. Lyubovitskij, Phys. Rev. D **80**, 054019 (2009)
7. R.M. Albuquerque, M.E. Bracco, M. Nielsen, Phys. Lett. B **678**, 186 (2009)
8. G.J. Ding, Eur. Phys. J. C **64**, 297 (2009)
9. J.R. Zhang, M.Q. Huang, J. Phys. **G37**, 025005 (2010)
10. Z.G. Wang, Eur. Phys. J. C **74**, 2963 (2014)
11. X. Chen, X. Lu, R. Shi, X. Guo, arXiv:1512.06483
12. M. Karliner, J.L. Rosner, Nucl. Phys. A **954**, 365 (2016)
13. A. Martinez Torres, K.P. Khemchandani, J.M. Dias, F.S. Navarra, M. Nielsen, arXiv:1606.07505
14. F. Stancu, J. Phys. **G37**, 075017 (2010)
15. N.V. Drenska, R. Faccini, A.D. Polosa, Phys. Rev. D **79**, 077502 (2009)
16. V.V. Anisovich, M.A. Matveev, A.V. Sarantsev, A.N. Semenova, Int. J. Mod. Phys. A **30**, 1550186 (2015)
17. Z.G. Wang, Y.F. Tian, Int. J. Mod. Phys. A **30**, 1550004 (2015)
18. R.F. Lebed, A.D. Polosa, Phys. Rev. D **93**, 094024 (2016)
19. N. Mahajan, Phys. Lett. B **679**, 228 (2009)
20. Z.G. Wang, Eur. Phys. J. C **63**, 115 (2009)
21. Z.G. Wang, Z.C. Liu, X.H. Zhang, Eur. Phys. J. C **64**, 373 (2009)
22. X. Liu, Phys. Lett. B **680**, 137 (2009)
23. E.S. Swanson, Phys. Rev. D **91**, 034009 (2015)
24. R. Aaij et al., arXiv:1606.07895
25. R. Aaij et al., arXiv:1606.07898
26. Z.G. Wang, arXiv:1606.05872
27. K.A. Olive et al., Chin. Phys. C **38**, 090001 (2014)
28. A. De Rujula, H. Georgi, S.L. Glashow, Phys. Rev. D **12**, 147 (1975)
29. T. DeGrand, R.L. Jaffe, K. Johnson, J.E. Kiskis, Phys. Rev. D **12**, 2060 (1975)
30. Z.G. Wang, Eur. Phys. J. C **71**, 1524 (2011)
31. R.T. Kleiv, T.G. Steele, A. Zhang, Phys. Rev. D **87**, 125018 (2013)
32. Z.G. Wang, Commun. Theor. Phys. **59**, 451 (2013)
33. Z.G. Wang, T. Huang, Phys. Rev. D **89**, 054019 (2014)
34. W. Chen, S.L. Zhu, Phys. Rev. D **83**, 034010 (2011)
35. H.X. Chen, E.L. Cui, W. Chen, X. Liu, S.L. Zhu, arXiv:1606.03179
36. Z.G. Wang, Commun. Theor. Phys. **63**, 466 (2015)
37. Z.G. Wang, Eur. Phys. J. C **74**, 2874 (2014)
38. Z.G. Wang, T. Huang, Nucl. Phys. A **930**, 63 (2014)
39. Z.G. Wang, Eur. Phys. J. C **70**, 139 (2010)
40. M.A. Shifman, A.I. Vainshtein, V.I. Zakharov, Nucl. Phys. B **147**, 385 (1979)
41. M.A. Shifman, A.I. Vainshtein, V.I. Zakharov, Nucl. Phys. B **147**, 448 (1979)
42. L.J. Reinders, H. Rubinstein, S. Yazaki, Phys. Rep. **127**, 1 (1985)
43. P. Pascual, R. Tarrach, *QCD: renormalization for the practitioner* (Springer, Berlin, 1984)
44. S.J. Brodsky, D.S. Hwang, R.F. Lebed, Phys. Rev. Lett. **113**, 112001 (2014)
45. Z.G. Wang, Commun. Theor. Phys. **63**, 325 (2015)
46. Z.G. Wang, Eur. Phys. J. C **76**, 387 (2016)
47. P. Colangelo, A. Khodjamirian, arXiv:hep-ph/0010175
48. S. Narison, Camb. Monogr. Part. Phys. Nucl. Phys. Cosmol. **17**, 1 (2002)
49. M. Gell-Mann, R.J. Oakes, B. Renner, Phys. Rev. **175**, 2195 (1968)
50. A. Khodjamirian, T. Mannel, N. Offen, Y.M. Wang, Phys. Rev. D **83**, 094031 (2011)